International Journal of Coal Geology 122 (2014) 61–75

Contents lists available at ScienceDirect

International Journal of Coal Geology

journal homepage: www.elsevier.com/locate/ijcoalgeo

Morphology and histochemistry of coalified *Trigonocarpus grandis* (Sydney Coalfield, Canada): Implications for the preservation, chemotaxonomy, and evolution of Carboniferous medullosalean ovules

Erwin L. Zodrow [a], José A. D'Angelo [a,b,*], Ahmad Al-Shra'ah [c]

[a] Carboniferous Palaeobiology Laboratory, Cape Breton University, Sydney, Nova Scotia, Canada
[b] IANIGLA-CCT-CONICET and Área de Química, Instituto de Ciencias Básicas, Universidad Nacional de Cuyo, Centro Universitario, M5502JMA Mendoza, Argentina
[c] Department of Chemistry, Memorial University of Newfoundland, Canada

ARTICLE INFO

Article history:
Received 27 September 2013
Received in revised form 9 December 2013
Accepted 9 December 2013
Available online 21 December 2013

Keywords:
Medullosalean
Ovules
Coalified
Chemistry
M/z ratios
Preservation

ABSTRACT

From seven of the eight studied coalified ovules (*Trigonocarpus grandis*: Sydney Coalfield, Canada) sufficient material could be macerated (Schulze's process) for histochemical investigation. This encompasses histological identification of the ovular structure/tissue components by methods of Nomarski phase-contrast microscopy, and determination of the chemical make-up by Fourier transform infrared (FTIR) spectroscopy. The generated data are then input for principal component analysis (PCA), based on the chemometric approach. Not included in PCA, but complementary to it, are data from pyrolysis gas chromatography/mass spectrometry (Py-GC/MS), powder X-ray diffraction, carbon 13 magnetic resonance analyses (^{13}CNMR), and introducing mass spectrometric data of selected epidermal/nucellar and vitrain samples. Addressed amongst other questions are evolution of ovular chemical grouping which includes vitrain and cutin; if coalified ovules reflect optimally original Carboniferous seeds, and why; and can chemotaxonomy/systematics of medullosalean ovules be advanced through histochemistry?

Demonstrably preserved in *T. grandis* are outer and inner integumentary epidermises, a double-walled nucellus with nucellar cuticles, and endospermous tissue. These structures are protected by tecta or nucellar cuticles. Molecular structures for epidermises and nucellii are probably not the same which is suggested by initial mass-spectrometric experiments. These "hard" parts are most resistant to diagenetic influences, correlating with aliphatic (lipid) composition, but facies changes influenced fossilization as in ovular molds/casts vitrain lost all its otherwise preserved tissues. This collectively suggests a narrow window of fossilizing conditions by coalification. Inferred from PCA are transitional changes, rather than sharp delineation, where the nucellus occupies a chemical composition intermediate between epidermis/cutin and the vitrain. Integumentary fibers, tectum, inorganic replacement of an epidermis, and some nucellar specimens are difficult to group by PCA. Nucellar material is probably suited for chemotaxonomic/systematic research because of the lipid chemistry.

1. Introduction

Studies of Carboniferous medullosalean compressions/cuticles are numerous (summaries: Cleal and Shute, 2012; Kerp, 1990), but rare for associated coalified ovules (cf. Van Bergen et al., 1994). Hooker and Binney (1855) mentioned compressed *Trigonocarpus* Brongniart from the Lancashire coal-field, England, and Deevers (1937) diligently sectioned trigonocarpalean seed casts (3–5 cm long and 2–3 cm wide) from Arkansas, U.S.A., without success for cellular detail.

Trigonocarpalean ovules are abundant in American (and European) Carboniferous localities of similar age (summary: Gastaldo and Matten, 1978), but rare in the Pennsylvanian-age Sydney Coalfield, Fig. 1A, B (cf. Bell, 1938, 1962). Dawson (1868, p. 437) claimed, however, abundance for these "fruits" in the Carboniferous of the Canadian Maritimes (Acadia). Nevertheless, twenty-three coalified ovules were collected by the senior author (ELZ) from Asturian–Cantabrian strata of the Sydney Coalfield. The "best" of these, indubitably referable to *Trigonocarpus grandis* (Lesquereux) (Cleal et al., 2010), included two ovules that separated into three major segments (Appendix A, supplementary material). Ovule 5-Lst#9, demonstrably of spectacular tripartite segmentation (Fig. 2), lacks the preservation detail of the second 2–336 ovule that provided the most complete up-to-date structural information of published coalified ovules (Fig. 3A–D). For this study, we benefitted from earlier experimental work with coalified *T. grandis* ovules concerning

* Corresponding author at: Instituto Argentino de Nivología, Glaciología y Ciencias Ambientales (IANIGLA)-CCT-CONICET-Mendoza, Avda. Ruiz Leal s/n Parque Gral. San Martín (5500) Mendoza, Argentina. Fax: +54 261 5244201.
E-mail addresses: Erwin_Zodrow@cbu.ca (E.L. Zodrow), joseadangelo@yahoo.com (J.A. D'Angelo), aalshraah@mun.ca (A. Al-Shra'ah).

0166-5162/$ – see front matter © 2013 Elsevier B.V. All rights reserved.
http://dx.doi.org/10.1016/j.coal.2013.12.008

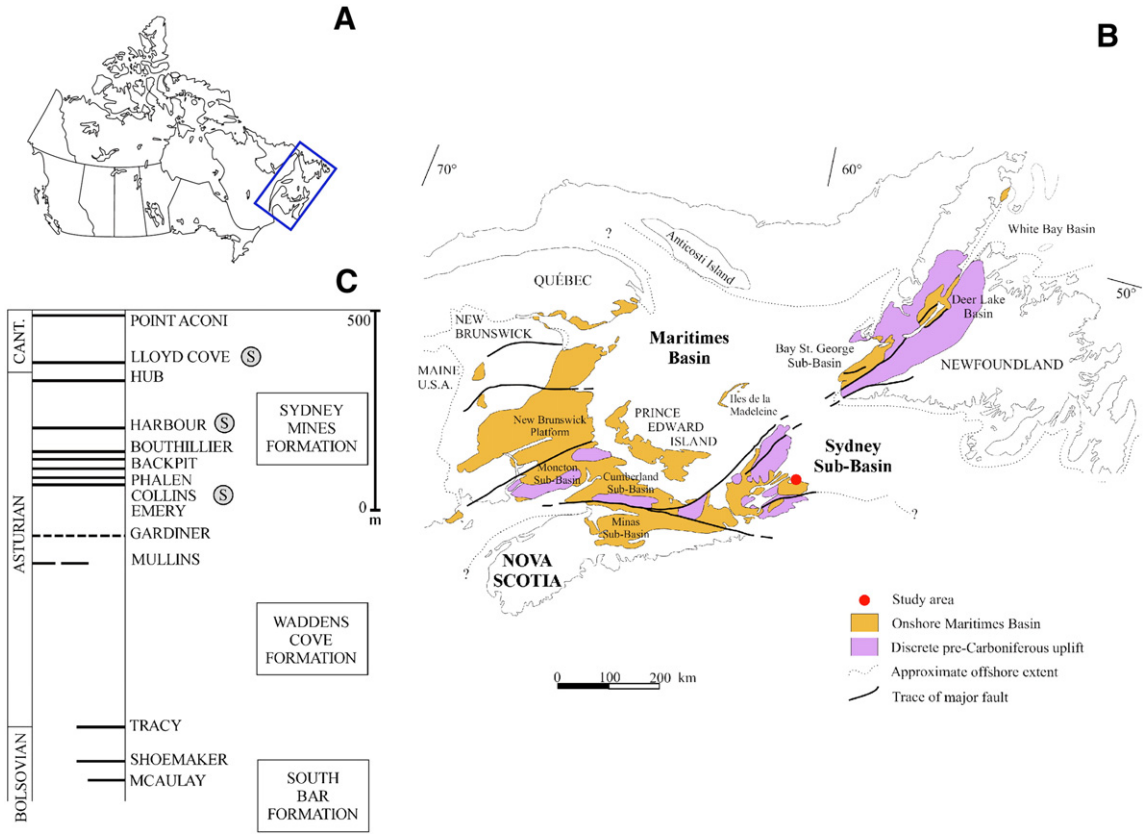

Fig. 1. Study location in Canada (A) and (B). (C) Coal lithostratigraphy in Sydney Coalfield. (S) Sampled coal seams; CANT. Cantabrian Sub-Stage.

the maintenance of the structural sequence of the seed while preparing histological slides (D'Angelo and Zodrow, 2011; Zodrow et al., 2013a).

Discussed and interpreted are results from the view points of optimal preservation summarized as a model for *T. grandis*, and chemical interrelationship of preserved ovular structures of use for the systematics of medullosalean ovules. The latter may have implication for the phylogeny of living cycads (cf. Norstog and Nicholls, 1997). Earlier terminology by Zodrow et al. (2013a) is revised.

1.1. Revising earlier nomenclature

Carboniferous-age fossil seeds of medullosalean tree-fern lineage (Hoskins and Cross, 1946a) basically comprise a seed-coat (integument) with epidermises for the nucellus, i.e., the megaspore membrane: Fig. 3C (summary: Herr, 1995; Zodrow et al., 2013a). All epidermises are protected by tissue referred to as tectum, analogous to an exine-roof cover (cf. Thomas and Spicer., 1987, Fig. 13.2), SEM-illustrated for medullosalean ovules by Zimmerman and Taylor (1970). Protection for the megaspore membrane is by nucellar cuticles. The outermost skin, i.e., the cuticle, though not preserved, is assumed stomatiferous (cf. Taylor, 1965), analogous to the living cycad seed Cycas *rumphii* (Zodrow et al., 2013b). Epidermal surfaces are either adaxial or abaxial to the outer or the inner integuments, where the reference is an imaginary medial-bisector plane (or axial trace) of the seed (marked MP: Fig. 3C). See Fig. 4 for nomenclature of cellular topography, i.e., outlines of boundaries: anticlines, and cross sections.

1.2. What is a coalified ovule?

At least three interrelated pathways of organic matter transformation are involved in coalified ovules, depending on the original make-up of the seeds. One of these leads to vitrain ("shiny coal", Stopes, 1919) composed of complex hydrocarbon molecules, a second to structure/tissue of cutin-like/wax biomacromolecular composition in the vitrain, and a third to nucellar preservation. Vitrain is soluble in an oxidizing solution of Schulze's process, whereas the structure/tissue components are not, but presumably solubilize in an ionic liquid (salt in the liquid state at room temperature, Novoselov et al., 2007; Teacă et al., 2011). The defining features of a coalified ovule (Fig. 3A, arrowed) rest with recoverable structure/tissue components from vitrain, particularly the nucellus, in a predictable succession (Fig. 3B).

2. Material, preservation types, samples, and methods

2.1. T. grandis ovules

Fig. 1C provides the lithostratigraphical background in Sydney Coalfield for the sample locations of these large ovules. Ovules 2–336, 5-Lst#9, Ovxx2, 3–309, 5–11-10–5, and 5-Lst#20 originated from the roof rock one to two meters above the Lloyd Cove Seam. This location is part of the Canadian Maritime medullosalean-forest lagerstatt with huge amounts of mostly alethopterid seed-fern foliage, but rare coalified ovules (Zodrow, 2002, 2007; Zodrow et al., 2013a; this study). Ovules 78–403a (Fig. 5A) and 4–261.

(Fig. 5B) originated from the roof rocks of the relatively older Harbour and Collins Seams, respectively.

The ovules are found isolated, in clusters, or in longitudinal arrays as if they were borne on an axis (Cleal et al., 2010; Doubinger et al., 1995; Zodrow, 2002, 2004, 2007, Figs. 247–248; and White, 1899, p. 267;). Where and how they are attached to the mother tree *Alethopteris pseudograndinioides* (Zodrow et al., 2013a) is debatable (Cleal et al., 2010; Mosbrugger, 1989).

2.1.1. Preservation types of T. grandis

The study ovules were entombed in three different lithologies, or facies: (1) unaltered shale at the Lloyd Cove Seam, (2) dark carbonaceous

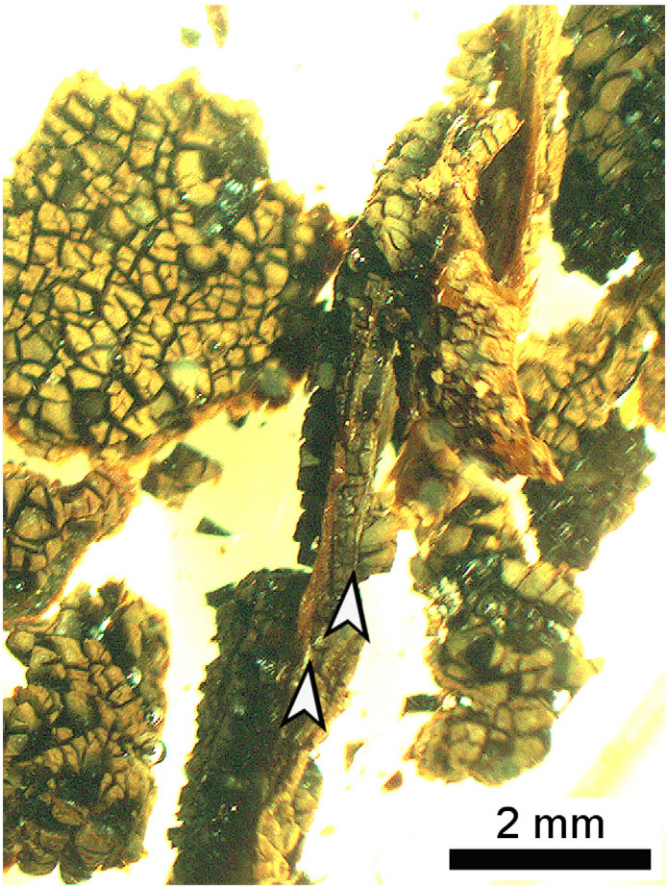

Fig. 2. *Trigonocarpus grandis*, 05-Lst#9 ovule. Real-time photography during premaceration capturing developing tripartite separation. Arrows point to the two nucellar traces, with the coalified endosperm preserved between them.

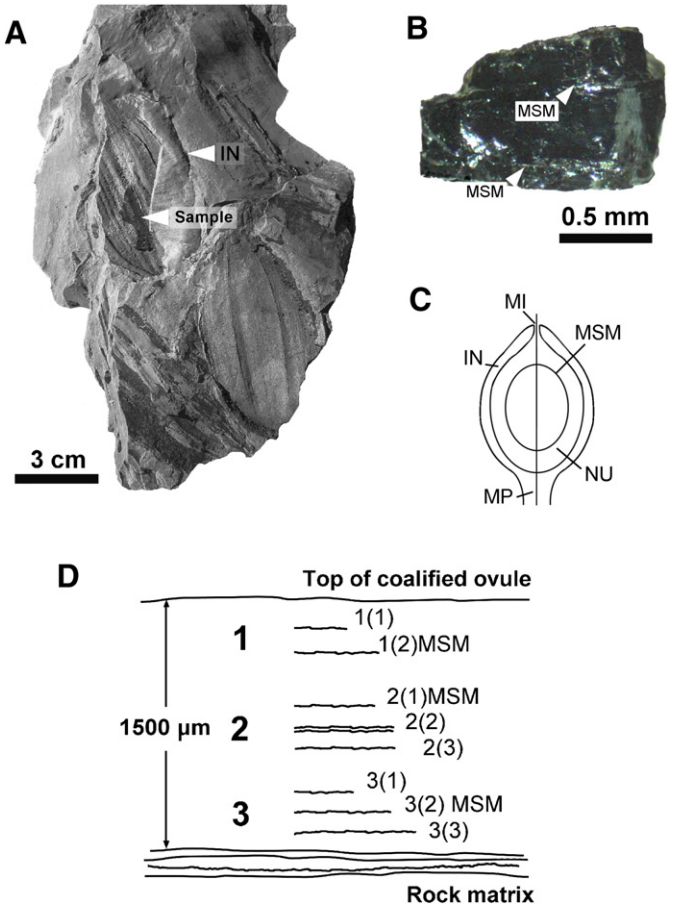

Fig. 3. *Trigonocarpus grandis*, 2–336 ovule hand specimen. (A) In situ coalified material remaining on the impression for analyses; IN integuments. (B) Close-up of the two central nucellar traces in the vitrain. (C) Simplified longitudinal cross section of an ovule. MI micropyle; NU nucellus; MSM megaspore membrane, and MP imaginary medial–bisector plane. See Truernit and Haseloff (2008), Fig. 2). (D) Numbering of the tripartite segments **1**, **2**, and **3** and subsegments **1**(1) to **3**(3).

siltstone/claystone/(FeII) carbonate (siderite) with abundant framboidal pyrite clusters as large as 300 µm in diameter at the Harbour Seam, and (3) clayey mudstone at the Collins Seam. Overall, they fossilized under near-equal and moderate temperature–pressure conditions, as attested to by lower vitrinite–reflectance values, hardly differing for the seams (Table 1). Three empirical preservation types are recognized:

Type(i) coalified ovules, which are slightly oval in cross section, 66–1900 µm thick, characterized by two central, parallel brownish nucellar complexes that are separated by a 50–200 µm thick vitrain band (endosperm), and composed of 7–8 vitrain bands. Specimen (ovule 5-Lst#9) is an instance of coal-ball-like inorganic chemistry. These ovules are known only from the Lloyd Cove Seam;

Type(ii) 3-D ovules (three dimensional preservation), which occur as mold/cast; nucellar complexes are not preserved. These ovules, found only at the Harbour and the Collins Seams, resemble *Trigonocarpus dawesi* Brongniart preservation described by Deevers (1937), Fig. 1), or *Trigonocarpus leeanus* Gastaldo and Matten, 1978. Sclerotestal dehiscence exposed three features (micropyle, seed concavity, and palisade structure) that are not preserved in the coalified ovules at the Lloyd Cove Seam; and

Type(iii) semi-coalified ovules, mostly known from the Collins Seam; they are flatly adpressed onto the rock matrix without preserved nucellar complexes, and the comprising 1–3 coalified layers are thin, 33–133 µm. Peculiar to the ovules of this type is an amber-colored tissue (e.g., Fig. 5B1 and B2) similar to a fossilized-cuticle (Zodrow and Mastalerz, 2009). However, delineating preservation boundaries concretely is not realistic. Rather, we believe that the preservation types are best conceptualized in a three-dimensional continuum as proposed by Zodrow and D'Angelo (2013), Fig. 2).

2.2. Material and methods

Appendix A (supplementary material) describes preparation of materials including maceration procedure, apportionment of samples for the various analytical methods used, long-term maceration treatment for certain ovular structures, and repository of the study material.

2.2.1. Nomarski phase-contrast microscopy

This method of microscopy is standard for fossil-histological studies, and taking cellular measurements which were made at ×250 magnification. However, as only smaller sample numbers are involved from smaller fragments, the intent is for circumscribing size ranges

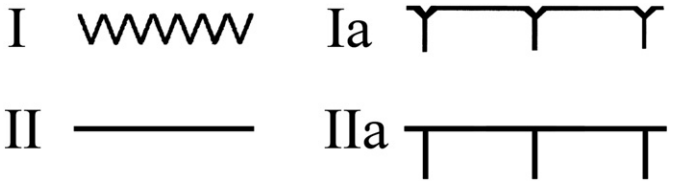

Fig. 4. Cellular borders I and II, and cross sections Ia and IIa. Source: Koch et al. (2009), Figs. 6–8).

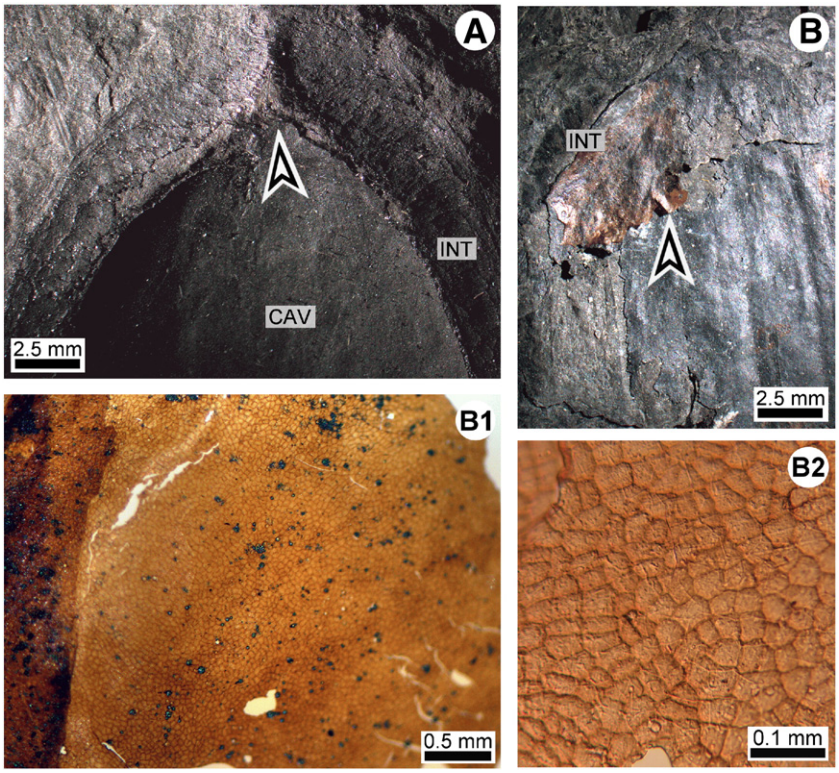

Fig. 5. *Trigonocarpus* sp. (A) 3-D ovule with pronounced central cavity CAV, integuments INT, and micropyle, arrowed. Harbour Seam, 78–403a. (B) Flatly adpressed ovule with longitudinal ribs. Naturally macerated epidermis, arrowed. (B1) Close-up of (B) left to the arrow. (B2) Epidermis, after macerating (B1) for 4 h. Nomarski phase-contrast photography. Collins Seam, 4–261.

(minimum–maximum). Accurate anticlinal widths were measured in the red phase-contrast spectrum that filtered out the cutinized borders of cells.

2.2.2. Solid-state FTIR

Details of the KBr-pellet method used for FTIR analyses, and references for the mathematical procedures involved in IR (infrared) processing techniques, are found in D'Angelo and Zodrow (2011). The tectal sample of barely minimum weight (0.5 mg) was prepared as a 200 mg KBr pellet for reliability, instead of the usual 250 mg KBr used. Definition of semi-quantitative IR-area ratios and their explanations are summarized in Table 2. Interpreting IR spectra is found in Lyons et al. (1995), Merk et al. (1998), Zodrow et al. (2009, 2012), Cheng et al. (2012), and others.

2.2.3. Surface fitting and chemometrics

Surface fitting, or a three-dimensional (3D) plot, is used to reveal hidden patterns of row data, and to detect relationships amongst the three variables CH_2/CH_3 ratio, 'A' factor and 'C' factor. A more comprehensive analysis of the FTIR data is by PCA (Appendix B, supplementary material) for evolving chemical groupings (functional groups) as a function of structure/tissue for which PCA scores are appropriate. The underlying principle is the chemometric method that relates measurements made on organic functional groups to the state of the system via PCA (cf.D'Angelo and Zodrow, 2011, 2013).

Table 1
Physical appearance of the ovules.

Specimen	Impression (cm)		Coalified material			Megaspore membrane		Roof-rock lithology	Vitrinite reflectance
(No. of slides) (Preservation type)[c]	Length	Width	Damage	Preserved[a] (cm)	Thickness (μm)	μm	μm	(Coal Seam)[b]	(Ro %)
Trigonocarpus grandis									
2–336(21)(i)	7	4	Slightly	3 × 1.5	1500–1667	33	66	Unaltered shale (Ll)	nm[d]
5-Lst#9(44)(i)	7	4	Major	3 × 3	750–1900	30–50	20–80	Unaltered shale (Ll)	0.76 ± 0.49 (n = 23)
Ovxx2(6)(i)	6	4	Slightly	4 × 3	nm[d]	nm[d]	nm[d]	Unaltered shale (Ll)	0.72 ± 0.04 (n = 8)
3–309(16)(i)	6	5	Slightly	3 × 2	1800	33	33	Unaltered shale (Ll)	0.72 ± 0.23 (n = 24)
5-Lst#20(22)(i)	7	5	Slightly	3 × 1	nm[d]	nm[d]	Missing	Unaltered shale (Ll)	0.71 ± 0.04 (n = 24)
5-11-10-5(9)(i)	6	3	Major	2 × 1	100–330	25	Missing	Unaltered shale (Ll)	nm[d]
Trigonocarpus aff. *grandis*									
78–403a(ii)	7–8	4	Slightly	na[e]	166	Not preserved		Carbonate/siltstone (H)	0.70[f]
4–261(1)(iii)	6?	3	Major	Not known	66–133	Not preserved		Clayey mudstone (C)	0.76[f]

[a] Approximate area of preserved coalified material.
[b] Coal Seam: (Ll) Lloyd Cove, (H) Harbour, (C) Collins.
[c] Preservation types: (i) coalified, (ii) 3-D, (iii) semi-coalified.
[d] Not measured.
[e] Not applicable.
[f] Hacquebard (1993), (Fig. 7).

Table 2
Definition of semi-quantitative area ratios derived from FTIR spectra.

Ratio	Band-region (cm^{-1})	Interpretation and remarks
	Band-region ratios	
CH_2/CH_3	3000–2800	Methylene/methyl ratio. It relates to aliphatic chain length and degree of branching of aliphatic side groups (side chains attached to macromolecular structure; Lin and Ritz, 1993a, b). Higher value implies comparatively longer and straight chains, a lower value shorter and more branched chains. Caution is advised using the ratio, as it may be misleading due to the contribution from CH_2 and CH_3 groups attached directly to aromatic rings (Petersen and Nytoft, 2006).
CH_{al}/Ox	(3000–2800)/(1800–1600)	Aliphatic/Oxygen-containing compounds ratio. Relative contribution of aliphatic C–H stretching bands (CH_{al}) to the combined contribution of oxygen-containing groups and aromatic carbon (Ox). From higher values decreasing oxygen-containing groups can be inferred, or the lower the CH_{al}/Ox ratio, the higher the Ox term. This ratio could provide some information about oxidation in organic matter (e.g., Mastalerz and Bustin, 1997; Zodrow and Mastalerz, 2001).
'A' factor $= CH_{al}/(CH_{al} + C=C)$	(3000–2800)/[(3000–2800) + (1650–1520)]	Relative contribution of aliphatic C–H stretching bands to sum of aliphatic C–H stretching and aromatic carbon structures. According to Ganz and Kalkreuth (1987) it represents change in relative intensity of aliphatic groups.
'C' factor $= Ox/(Ox + C=C)$	(1800–1600)/[(1800–1600) + (1650–1520)]	Relative contribution of oxygen-containing compounds to sum of oxygen-containing structures and aromatic carbon bands. According to Ganz and Kalkreuth (1987) it represents change in carbonyl/carboxyl groups.
$CH_{al}/C{=}O$	(3000–2800)/(1800–1700)	Aliphatic/carbonyl groups ratio. Relative contribution of aliphatic C–H stretching bands to carbonyl/carboxyl groups (C=O). Indicator for cross-linking degree of a polymeric structure. Lower values indicate higher C=O content and higher cross-linking (Benítez et al., 2004).

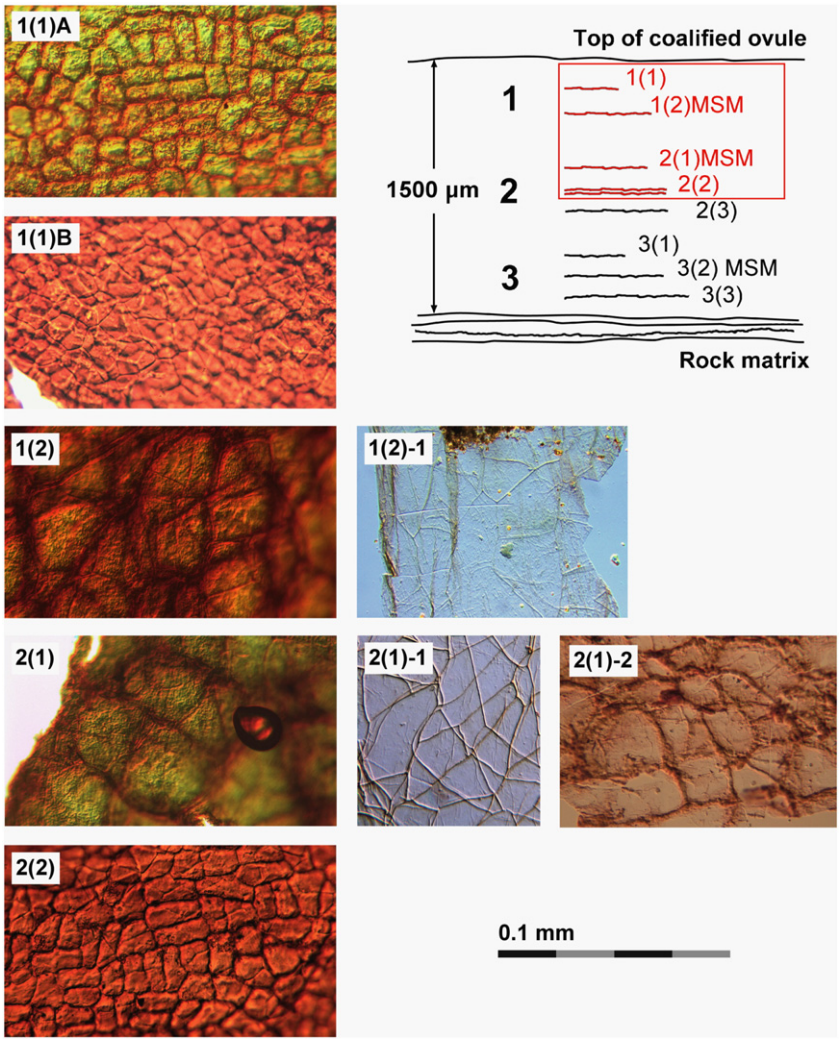

Fig. 6. *Trigonocarpus grandis*. Structure/tissue documentation of 2–336 ovule. See text for details.

2.2.4. Py-GC/MS

Pyrolytical techniques can provide valuable semi-quantitative information, even with condensed, insoluble macromolecular materials that cannot be completely isolated from the mineral matrix without chemical alterations. It is also used to confirm FTIR interpretation. Flash pyrolysis of 0.35 mg of the three nucellar samples [Figs. 6 and 7: **1(2)**, **2(1)**, and **3(2)-1: the coaly part,** respectively], and subsequent analysis of the pyrolysates were carried out using a Frontier Lab vertical micro-furnace at 600 °C. It was interfaced to an HP gas chromatography/mass spectrometer (GC/MS) with a 30 m by 0.25 mm (25 μm thickness) DB-1701 capillary column. All interface temperatures were at 260 °C, theGC oven program was 35 °C (initial) to 265 °C at 7 °C/min ramp. Identity of the peaks was verified using standards and mass-spectrum library matchings. This method compares with using separate low-and high-molecular pyrolysates (cf. Zodrow et al., 2013a).

2.2.5. Cutin analysis

Nucellar and epidermal specimens from Ovxx2 ovule were macerated for nearly three weeks, and Indiana paper coal for one week. The experimental rationale behind this approach is an attempt to concentrate cutin, because the signature of it are higher levels of the CH_2/CH_3 ratio (aliphatics), analogous to the ratios obtained for Carboniferous foliage (cf. D'Angelo et al., 2013; Stoyko et al., 2013; van Bergen et al., 2004). The treated Indiana paper coal served as cutin comparison (Neavel and Miller, 1960; Nip et al., 1989).

2.2.6. Mass-to-charge ratio (m/z)

Waters Atmospheric Solids Analysis Probe (ASAP) sampling technique, coupled with Xevo G2 QT mass spectrometer, was used to obtain m/z ratios (Pavia et al., 2009) from vitrain of the Lloyd Cove seam and from 3–309 ovule, and from epidermal and nucellar samples (Appendix A, supplementary material). In comparison with minimum sample requirement of 0.5 mg for IR analysis, ASAP uses a tiny fraction of it which heated nitrogen desolvation gas (450 °C) vaporized and a corona discharge ionized to obtain the spectrum in the range of 50–1100 m/z. Mass spectrometry, in addition to currently used technologies (e.g., Zodrow et al., 2013a), is a promising technique for attempting to circumscribe biomacromolecular parameters of fossil-cutin preservation, and consequently chemotaxonomic utility (cf. Kolattukudy, 2002).

3. Results

3.1. Structure/tissue components of T. grandis

3.1.1. Ovule 2–336: type(i) preservation

Structure/tissue components in the three main segments of 2–336 ovule, bracketed **(1)** to **(3)**, are designated **1(1)A** to **3(3)**,

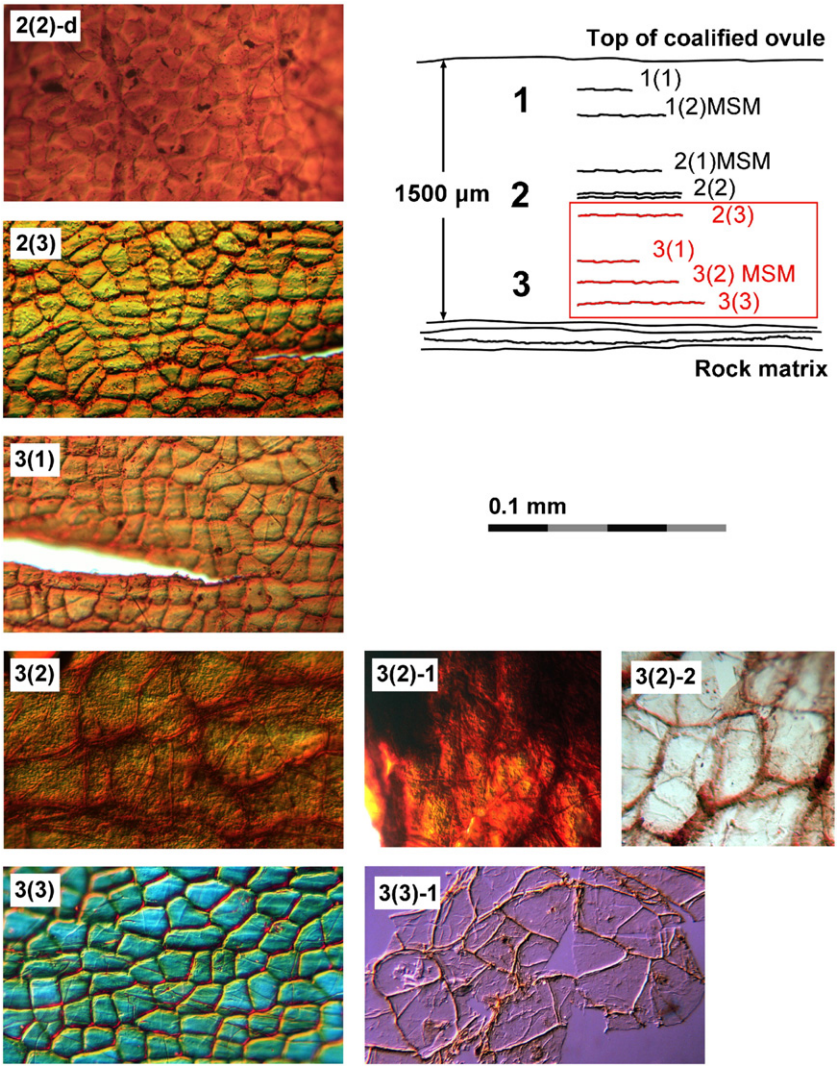

Fig. 7. *Trigonocarpus grandis.* Structure/tissue documentation of 2–336 ovule. See text for details.

Table 3
Data matrix of semi-quantitative FTIR ratios, and explanation of associate names, color-keyed to Fig. 11.

Name	CH_2/CH_3	CH_{al}/Ox	$CH_{al}/C{=}O$	'A' factor	'C' factor	Name	CH_2/CH_3	CH_{al}/Ox	$CH_{al}/C{=}O$	'A' factor	'C' Factor
2–336 ovule Lloyd Cove Seam											
Epidermis						Nucellus					
1(1)A	9.6	0.64	4.1	0.95	0.82	–	–	–	–	–	–
–	–	–	–	–	–	1(2)	9.1	1.03	8.7	0.94	0.65
–	–	–	–	–	–	2(1)	7.8	0.90	7.0	0.90	0.56
2(2)	6.4	0.61	3.9	0.89	0.67	–	–	–	–	–	–
2(3)	11.4	0.52	2.9	0.88	0.71	–	–	–	–	–	–
Sec. sample	8.0	0.50	3.9	0.86	0.61	–	–	–	–	–	–
3(1)	8.6	0.51	2.8	0.90	0.76	–	–	–	–	–	–
–	–	–	–	–	–	3(2)	10.4	0.92	6.2		
–	–	–	–	–	–	3(2)-1coaly[a]	11.6	0.86	5.2		
3(3)	13.5	0.67	3.7	0.92	0.76	–	–	–	–	–	–
336	10.8	0.68	4.6	0.87	0.60	–	–	–	–	–	–
–	–	–	–	–	–	336	9.5	1.21	10.6	0.94	0.61
AVERAGE	9.8	0.56	3.7	0.90	0.70	AVERAGE	9.7	0.98	7.5	0.92	0.63
05-Lst#9 ovule Lloyd Cove Seam											
Top	87.5	0.63	3.4	0.91	0.76	–	–	–	–	–	–
Carb	2.8	0.72	232	0.52	0.005	–	–	–	–	–	–
Bot	60.6	0.85	5.2	0.91	0.66	–	–	–	–	–	–
–	–	–	–	–	–	Nuc1	17.4	0.89	3.2	0.93	0.81
–	–	–	–	–	–	Nuc2	3.3	1.15	7.8	0.88	0.48
Fib	3.1	0.13	2.9	0.27	0.11	Fibers, macerated from the outermost vitrain					
V1	1.1	0.41	448.8	0.38	0.0014	Outermost vitrain					
V2	1.1	0.41	4154.1	0.37	0.0001	Second sample of the outermost vitrain					
V3	1.2	0.31	654.1	0.32	0.0007	Inner vitrain, nucellus removed					
V4	0.8	0.32	nc[b]	0.33	0.00	Second sample, inner vitrain nucellus removed					
Vitrain, Lloyd Cove Seam											
Vc	0.9	0.54	258.4	0.41	0.003	Sampled coal seam					
Vc1	0.8	0.40	20.5	0.35	0.026	Sampled coal seam					
3-309 Ovule, Lloyd Cove Seam: tectum and nucellus											
–	–	–	–	–	–	Nuc3	10.4	0.42	3.9	0.62	0.30
Tc	1.8	0.52	14.6	0.48	0.06	Physically peeled from the nucellus					
5-Lst#20 ovule, Lloyd Cove Seam											
Top12	14.7	0.49	9.7	0.62	0.14	–	–	–	–	–	–
05-11-10-5 ovule, Lloyd Cove Seam											
TopBot	33.4	0.65	4.9	0.80	0.44	–	–	–	–	–	–
4-261 Ovule, Harbour Seam											
261HF	7.9	1.16	44.6	0.80	0.08						
2614h[c]	0.6	0.35	272.3	0.46	0.00						
Cutin analysis: Ovxx2, Lloyd Cove Seam											
–	–	–	–	–	–	Ov11d[c]	6.1	0.76	3.6	0.88	0.67
–	–	–	–	–	–	Ov19d[c]	20.2	0.48	1.0	0.86	0.86
OvB19d[c]	8.4	0.25	0.4	0.87	0.94	–	–	–	–	–	–
Cutin analysis: Indiana paper coal 8d											
K1	84.1	0.30	0.7	0.87	0.90	–	–	–	–	–	–
K2	56.6	0.29	0.7	0.85	0.88	–	–	–	–	–	–

[a] Coaly part of the contiguous nucellus.
[b] Not calculated, C═O is zero.
[c] Hours (h), days (d) of maceration.

where **1(2)-1** for example refers to a cover (Figs. 6 and 7). These are keyed to the FTIR data set (Table 3), though data for the epidermis **1(1)B**, and cutinized nucellar cuticles could not be obtained for lack of sufficient sampling material. Ranges for cellular dimensions are summarized in Table 4.

1(1)A Epidermis, abaxial outer integument in contact with the rock matrix; relative top. Observed are near-isodiametric and larger rectangular shaped, where the rectangles occur haphazardly as singlets, doublets, or as quadruplets without a discernible pattern. The convex cells of these configurations have pronounced sunken anticlinal walls and V-undulating boundaries (Fig. 4I, Ia), a cutinized anticlinal field of ca. 6 μm width forms the margins, but the anticlinal width is only 1–1.5 μm.

Clearly seen when not focused on it is a tectal cover. It shows tabular cells with straight 1–1.5 μm wide anticlines (Fig. 4II, IIa) that are not cutinized; hence it lacks the wide cutinized anticlinal fields.

1(1)B Abaxial and adaxial epidermises of the inner integument. Overlapping edges clearly identify two surfaces which cannot be teased apart, and consequently a cell-wall diffusion is seen. Near-isodiametric cells predominate, though some rectangular singlets and doublets are present. The second surface is manifest by faint yellowish outlines of the cellular borders, but accurate measurements of them are not possible.

In addition, when racking-up the microscope, a cellular structure without luminae comes into focus, presumably an overprint that is comprised of rectangular (singlets, doublets, triplets, and quadruplets), and

Table 4
Summary of ranges of cellular dimensions (μm), and presence of single to octuple blocks of rectangular cells.

	Cellular ranges				Rectangles arranged as singlets (1) to octuplets (8)							
	Near-isodiametric		Rectangular									
	Width	Length	Width	Length								
2–336 ovule (Figs. 6 and 7)			Epidermal integument									
1(1)A OUTER	33–44	33–44	33–39	66–87	1	2	–	4	–	–	–	–
1(1)B INNER	26–43	43–67	27	67	1	2	–	–	–	–	–	–
overprint	43–67	50–74	33–70	0–123*	1	2	3	4	–	–	–	–
3(3)		30–57	33–67	26–47	53–87	1	2	3	4	–	–	–
Overall	26–67	33–74	26–70	53–123								
			Epidermal endosperm									
2(2) OUTER	26–57	40–67	16–44	44–100**	1	2	3	–	–	–	–	–
3(1) OUTER	33–50	37–54	33–54	60–80	1	2	3	4	5	6	7	8
Overall	26–67	37–67	16–54	44–100								
2(2)d INNER	30–54	30–57	27–57	47–84***	1	2	–	–	5	–	–	–
2(3) INNER	33–54	40–54	27–50	50–84	1	–	3	4	–	–	–	–
Overall	30–54	30–57	26–70	47–123								
			Tectum									
1(2)	84–134	84–150	33–84	103–234	Not applicable							
2(1)	74–100	87–100	67	100–167								
3(1)	–	67–100	67100									
3(3)	100–117	34–40	74–90									
Overall	74–134	84–150	33–100	67–234								
5-Lst#9 ovule (Fig. 9C1 and E, respectively)												
OUTER	10	10–50	24–44	68–100	1	–	–	–	–	–	–	–
INNER (carbonate-like)	30	60	–	–	–	–	–	–	–	–	–	–
4-261 ovule (Fig. 5B1)												
	23–44	27–50	27	55	–	2	–	–	–	–	–	8

Combined ranges of rectangular configurations:
*Singlet 40 × 123 **34–57 47–84 ***16–33 44–94.
Doublet 70 × 100 27–54 16–37 47–67.
Triplet 37 × 60 20–44 44–100.
Quadruplet 33 × 60.
OUTER and INNER integuments.

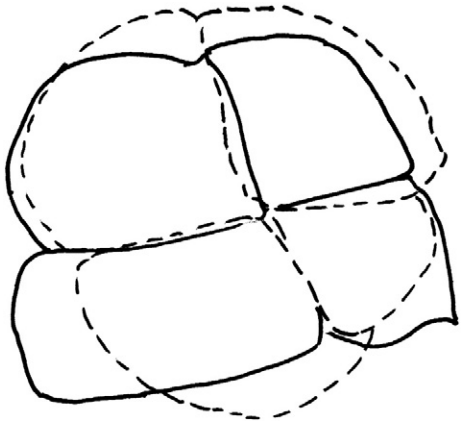

Fig. 8. Overlay of the nucellar cuticle, solid line, and its imprint on the nucellus (broken line).

near-isodiametric cells. Anticlines are straight, non-cutinized, and ca. 1–1.5 μm wide. Phenomena of this sort are expected, given the lithostatic loading pressure on the seeds since Carboniferous burial (Zodrow et al., 2013a).

1(2) Single megaspore membrane. The surface appears "muddied" caused by the adhering cutinized nucellar cuticle (thicker walls) and tectal debris, but the granular (exine) surface is clearly seen (cf. Darrah, 1968, Pl. 2, Fig. 8; Zimmerman and Taylor, 1970, Pl. 2, Figs. 3, 4; Zodrow et al., 2013a).

1(2)-1 Tectum. In addition to the above-mentioned characteristics, tecta adhere loosely to structures they cover, and luminae are very thin, as shown by negligible phase difference with the glass slide. From the undistorted tectal tissue, unbiased measurements for rectangular- and isodiametric-shaped cells could be recorded.

2(1) Single megaspore membrane. In contrast with **1(2)**, a clean exine surface was obtained since covering materials could be scraped off by hand. Overprints of nucellar cuticles, when not distorted, are ca.100 by 200 μm in size.

2(1)-1 Folded tectum, somewhat distorted.

2(1)-2 Cutinized nucellar cuticle with adhering tectum.

Fig. 8, based on **2(1)** and **2(1)-2**, demonstrates the fit of a nucellar cuticle on the nucellus, as already observed by Arnold (1948) for cutinized *Trigonocarpus* sp. in the Michigan Basin, U.S.A.

2(2) to 3(1) inclusive, are interpreted as endodermal double tissues; see Fig. 2 for the position of the vitrain-preserved endosperm.

2(2) Epidermis, outer abaxial. Two morphologies are present one with rectangular and the other with near-isodiametric cells. In addition, an epidermal overprint is visible with 1–1.5 μm wide anticlinal walls that are without anticlinal fields. A tectum is not observed.

2(2)d Epidermis, inner adaxial. Reliable measurements of the near-isodiametric and rectangular cell topography are difficult to obtain. A tectal cover is faintly visible.

2(3) Opposite to 2(2)d. Though rectangular doublets appear relatively frequent, occasionally forming a row connected by the short axis, singlets, triplets and a few quadruplets occur. Near-isodiametric cells are present, and a tectum is faintly visible.

Fig. 9. *Trigonocarpus grandis*, 5-Lst#9 ovule. (A) Real-time photography when macerating the outermost vitrain layer that literally sticks to the epidermis "Ct", where "A1" is the IR-spectrum of vitrain "A1" without the epidermis: see (A). (B) Fibrous material macerated from a vitrain fragment, e.g., "B" in (A), where (B1) is the IR-spectrum. (C1) Epidermis, see "C1" in (A). (D) Pointed, elongate cells, sclerotesta-related, where tectal tissue is slipping off during slide preparation (lower left border). (E) "Honeycomb-like" epidermal structure. In situ photography.

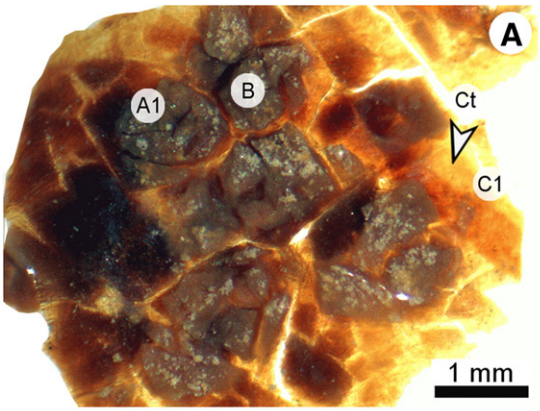
A
A1
B
Ct
C1
1 mm

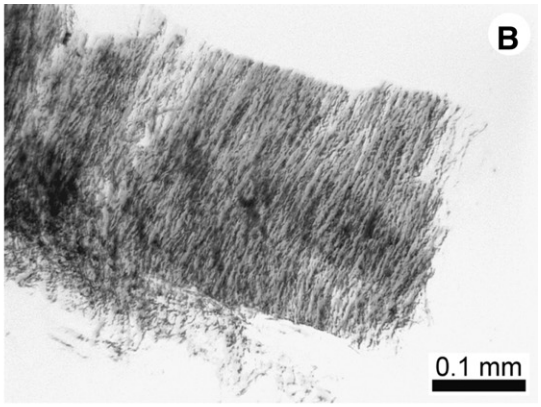
B
0.1 mm

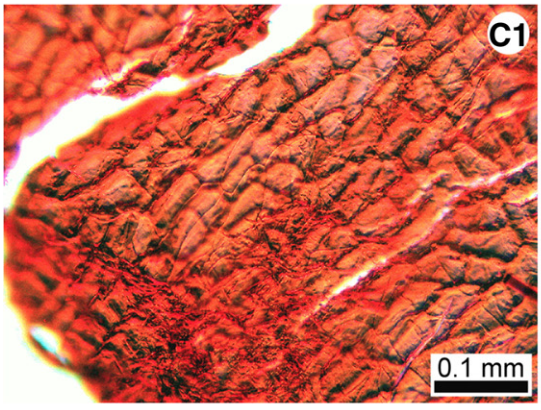
C1
0.1 mm

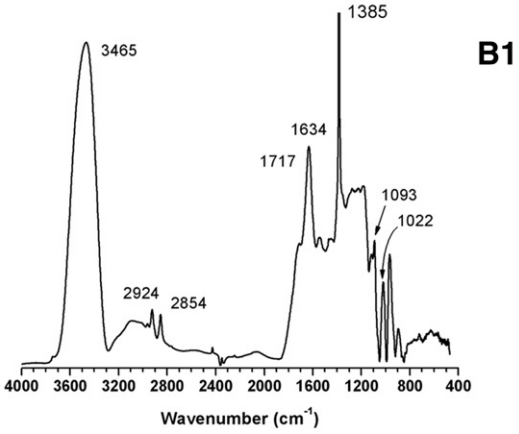
B1
3465
2924
2854
1717
1634
1385
1093
1022
4000 3600 3200 2800 2400 2000 1600 1200 800 400
Wavenumber (cm-1)

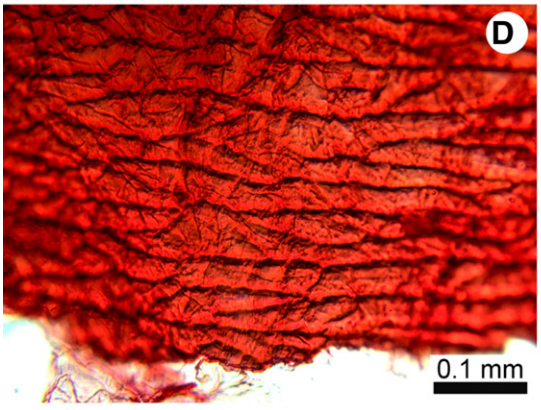
D
0.1 mm

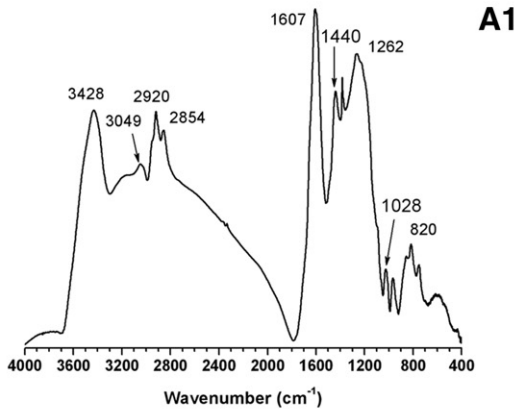
A1
3428
3049
2920
2854
1607
1440
1262
1028
820
4000 3600 3200 2800 2400 2000 1600 1200 800 400
Wavenumber (cm-1)

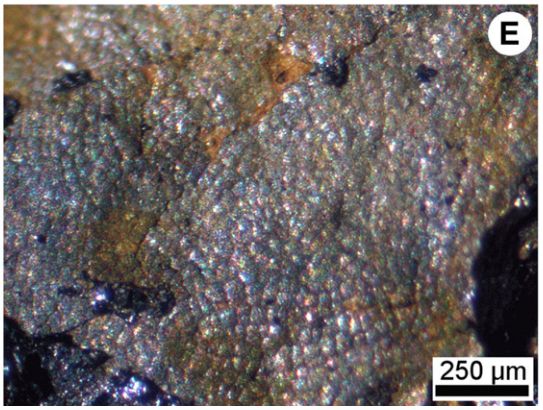
E
250 µm

3(1) Opposite to 2(2). The epidermis has the most varied arrangements of rectangular forms, from singlets to octuplets, and the second topography comprises near isodiametric cells. A tectal cover is clearly visible.

3(2) Single megaspore membrane. Similar to **1(2), 2(1)** in all aspects.

3(2)-1 Megaspore membrane is contiguous with **3(2)**, except that it has coaly aspects.

3(2)-2 Nucellar cuticle is at places undistorted; measurements of these large, near-isodiametric, cutinized cells are 100–134 μm by 117–200 μm. A cluster of round, smooth structures (not shown) are preliminarily interpreted as laevigate spores (13 μm in diameter) (cf. Hoskins and Cross, 1946b; Taylor, 1965).

3(3) Epidermis, outer integument in direct contact with the rock matrix. Relative bottom. Two cell topographies are observed. One is composed of rectangular singlet, doublet, triplet, or quadruplet forms, and the other of the near-isodiametric form.

3(3)-1 Tectum with some adhering cutinized nucellar membrane.

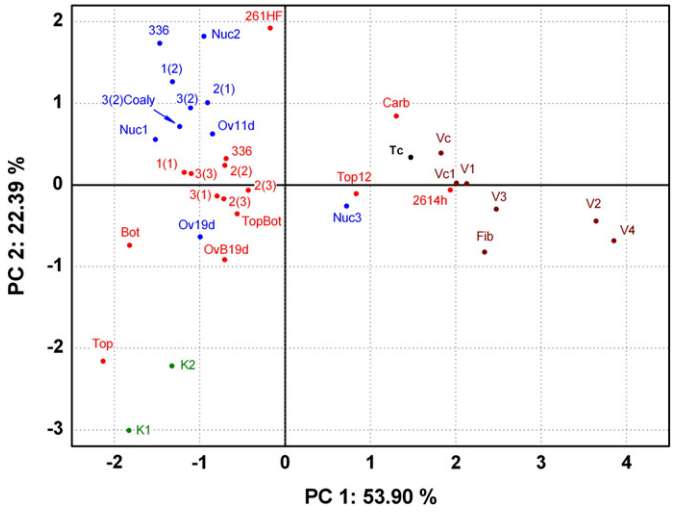

Fig. 11. Plot of principal-component scores (n = 35). Color key: Blue = nucellus, Red = epidermis, Light brown = vitrain, Black = tectum, Green = cutin.

3.1.2. Ovule 5-Lst#9: type (i) preservation

It is represented by maceration products from fragments marked "B", "C1" and "Ct" that are documented parts of an outermost ca. 300-μm thick vitrain fragment (Fig. 9A). The spectrum of the vitrain fragment "A1" is shown in Fig. 9A1. Another fragment "B" yielded a fibrous structure (Fig. 9B) whose IR spectrum is shown in Fig. 9B1 for comparison with the vitrain. The fibers are ca. 300 μm long and 3 μm wide, non-segmented, transparent, and oriented with the long axis orthogonally to the abaxial surface of the outermost epidermis (Fig. 9C1, "Ct" on Fig. 9A). Associated with the ca. 300-μm thick vitrain fragment is an unoriented, sclerotesta-related structure that is composed of pointed, elongate cells (max. 27–134 μm: Fig. 9D). Tecta are present, except on the fibers. Moreover, a carbonate-like epidermis (Fig. 9E), situated directly below the vitrain fragment, is composed of dome-shaped cells, ca. 30 μm by 60 μm in size with 3–6 μm wide anticlinal fields.

3.1.3. Ovules 78–403a and 4–261: type(ii) and type(iii) preservations

Ovule 78–403a shows two longitudinal ribs, though one is barely visible in the 2-cm wide seed cavity, which together with its size, points to affinity with *T. grandis* (Fig. 5A). The micropyle is ca. 30 μm in diameter and 1 mm long, and the seed cavity preserved a 166-μm thick, smooth coaly layer (sarcotesta) whose samples solubilized during maceration without yielding cellular products. A 4–5 mm wide coaly rim that preserved dense linear, and meshing curvilinear, transverse markings compares with palisade structure (cf. Oliver and Scott, 1904, Pl. 5, Fig. 11; Deevers, 1937, Fig. 35; de Sloover, 1964; Gastaldo and Matten, 1978). Macerated samples did not yield any cellular products.

Ovule 4–261, Fig. 5B, grouped with *T. grandis* because of three longitudinal ribs (cf. Deevers, 1937) appears to preserve the micropyle. The number of eroded coaly sub-layers is indeterminate which precludes ascertaining in the seed the structural position of the amber-colored "fossilized-epidermis" (Fig. 5B1); suggested is an outer integumentary position. Fig. 5B2 shows near-isodiametric and rectangular cells. The dimensions of both morphologies are smaller than epidermal cells

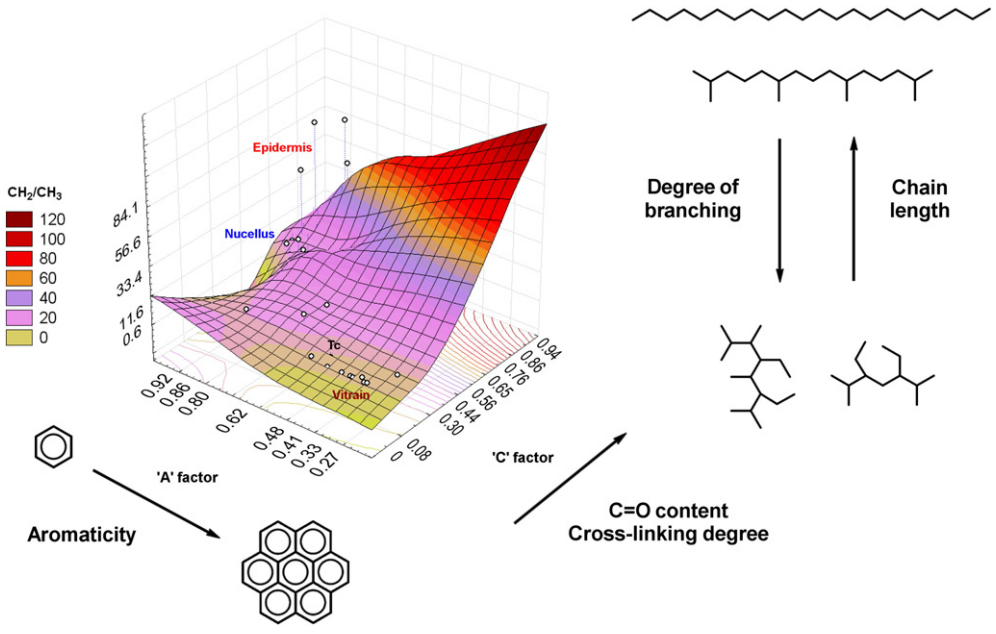

Fig. 10. 3D plot. Color key: Blue = nucellus, Red = epidermis, Light brown = vitrain, Black = tectum, Green = cutin.

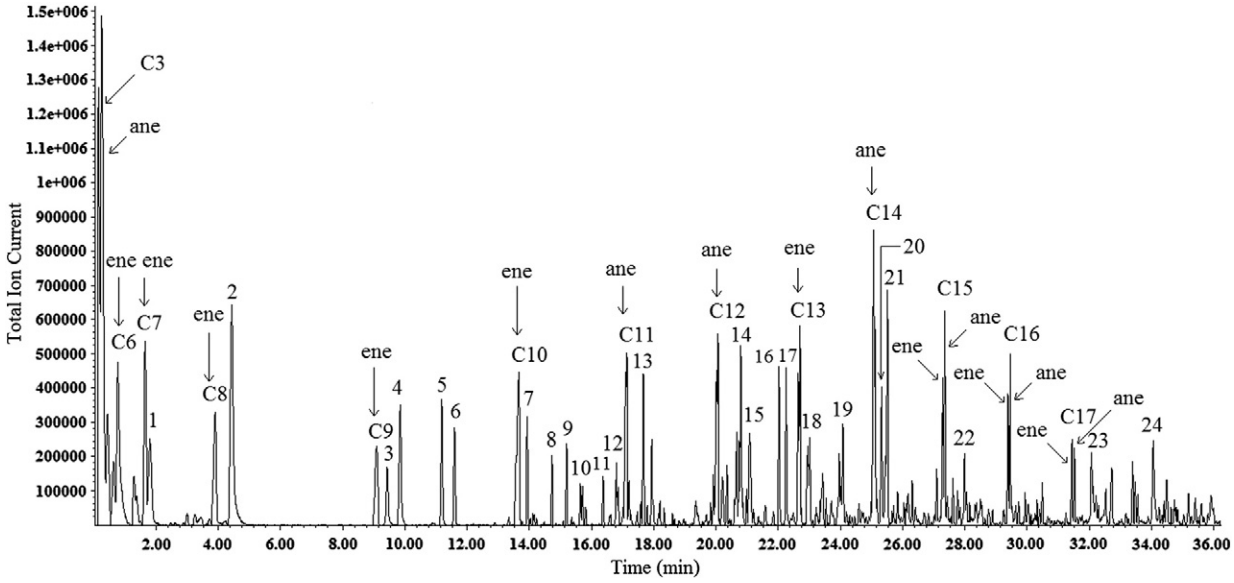

Fig. 12. *Trigonocarpus grandis*, 2–336 ovule. Py-GC/MS total-ion chromatogram of one of the three nucellii, i.e., 2(1) of Fig. 6.

(Table 4). Overprints of anticlinal walls, not focused on, are 1–1.5 μm wide and delineate larger cells (roughly 40 μm by 67 μm).

3.2. Surface fitting and PCA scores

A three dimensional plot (3D surface, Fig. 10) is used to reveal hidden patterns of IR data and to detect relationships amongst three variables: CH_2/CH_3 ratio, 'A' factor and 'C' factor. This is done as a function of the chemical structures (functional groups), and the calculated surface is color-shaded which corresponds to the z-axis values (CH_2/CH_3), where the projected contours are shown on the 'A' factor–'C' factor horizontal plane.

A more comprehensive analysis of the five variables describing the chemometric system (i.e., CH_2/CH_3, CH_{al}/Ox, 'A'factor, 'C'factor and $CH_{al}/C=O$) resulted into a two-component solution accounting for 76.28% variance. This assumes statistical redundancy of three components (Appendix B, supplementary material). The plot of the two-component scores is shown in Fig. 11.

3.3. Cutin analysis

The prolonged oxidative process turned the original brownish-looking specimens into whitish masses, exhibiting semi-metallic luster, that have lost all semblance to their respective original morphologies, similar to cutin of the Carboniferous foliage of *Macroneuropteris scheuchzeri* or *Alethopteris pseudograndinioides* (D'Angelo et al., 2013; Stoyko et al., 2013, respectively). The nucellar and epidermal samples of ovule Ovxx2, namely "Ov19d" (blue and red) and "Ov11d" (blue), do not plot with the Indiana paper coal that shows high CH_2/CH_3 ratio of 56 and 84 (Fig. 11 "K1 and K2", colored green). However, the outermost epidermis of 5-Lst#9, "Top", with the highest CH_2/CH_3 ratio of 87.5 does.

3.4. Py-GC/MS nucellar pyrolysates

Shown is only one chromatogram (Fig. 12), as the major pyrolysates and their relative abundances are strikingly similar to the other two nucellar samples (Table 5). One megaspore sample, **3(2)-1: the coal part,** is blackened but otherwise chemically similar to the two non-blackened nucellar parts of **1(2)** and **2(1).** This may be the result of fusion of the remnant integument with the nucellus (Reed, 1939; Stopes, 1905; Taylor, 1965), assuming integumentary tissues coalified.

All three chromatograms show *n*-alkene/*n*-alkane between C_{15}–C_{17}. Higher carbon-number aliphatic products would likely be observed if a less polar column were used. In contrast, total absence of alkene/alkane pairing is noted, instead alkanes were absent between C_3–C_{11}. The alkenes may indicate the presence of degraded lipid or fatty acid material. The abundant aromatic pyrolysates, those being C_0–C_3 alkylbenzenes and C_0–C_2 alkylphenols, are most probably markers of matured lignin components present in the sample. These pyrolytic chemical features were also observed by Edwards et al. (1997, and references there in) who performed analytical pyrolysis of the outer cortical tissue in Lower Devonian *Psilophyton dawsonii*. Finally, pyrolysis released a whole range of aromatic compounds, e.g., benzenes or 2-naphthanol (Table 5) which are probably derived from heavily altered aromatic biomacromolecules, or from secondary aromatization of diagenetic structures (Almendros et al., 2005).

Table 5
Py-GC/MS aromatic products of megaspore membranes of 2–336 ovule (e.g. Fig. 12).

Peak no.	Compound	Peak no.	Compound	Peak no.	Compound
1	Benzene	9	2-Propenylbenzene	17	Naphthalene
2	Toluene	10	1,3,5-Trimethylbenzene	18	4-methylphenol
3	Ethylbenzene	11	2,3-Dihydoindene	19	2,4-dimethylphenol
4	1,3-Dimethylbenzene	12	1H-indene	20	2-phenoxyethanol
5	1,4-Dimethylbenzene	13	1-Methyl-4-(1-methylethenyl)benzene	21	1,4-Dimethylnaphthalene
6	Ethenylbenzene	14	Phenol	22	1,4-Dimethylnaphthalene
7	1-Ethyl-2methylbenzene	15	3-Methyl-1H-indene	23	9H-fluorene
8	(1-Methylethyl) benzene	16	2-Methylphenol	24	2-Naphthanol

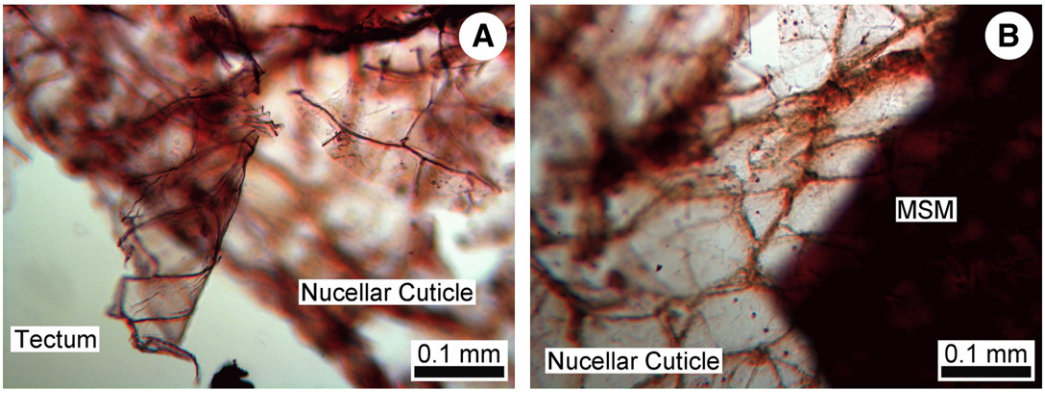

Fig. 13. *Trigonocarpus grandis*, 2–336 ovule. (A) and (B) represent a contiguous specimen. (A) The tectum is partially peeled-off the nucellar cuticle. Slide 2-336/5 × 10 3(2). (B) Nucellar cuticle in contact with the thick (dark) megaspore membrane MSM (nucellus). Slide 2-336/5 × 10 3(2) nuc cut.

3.5. Mass-to-charge ratios

Vitrain (spectra are not shown) of the Lloyd Cove Seam is presented by an m/z of 161 as is the vitrain of the 3–309 ovule, though the latter shows two additional low-intensity peaks (179 and 193). Nucellar and epidermal m/z's of 3–309 ovule are more complex. Whereas the former shows three peaks at 113, 120, and 125, the later shows a plethora of them in the range of m/z 170 to 209, with a high-intensity peak at 193.

4. Discussion

4.1. The "coalified hand-specimen model"

This refers to type(i)-preserved ovules, where the 7–8 vitrain sub-layer development is not considered a spurious phenomenon. Rather, it signals loss of cohesion between the tecta and vitrain during the maceration process (Zodrow et al., 2013a, Fig. 3B). Thus, on empirical evidence, fewer than 7–8 vitrain sub-layers, or fewer than two-double laminate megaspore membranes as in **3(2)**, see measurements in Table 1, would signal an incomplete coalified type(i) preservation.

4.2. Morphologies and model of structural sequence

Epidermal components are characterized by near-isodiametric and rectangular cells, without a repeating *motif* which leads us to hypothesize random cellular divisions. A 3 cm by 0.8 cm epidermal fragment (slide Ovxx2/4, 5), the largest specimen we have, confirmed the hypothesis. Implied is that the epidermal surfaces of *T. grandis* offer little or no taxonomic utility (cf. Zodrow et al., 2013a), which is also probably the case for other medullosalean ovules. Cellular borders of nucellar cuticles impressed upon the nucellus (e.g., Fig. 8) can be weak to strong, and judging from the size variation, the nucellus–cuticle cells had considerable size plasticity, probably as a function of location on the large nucellus.

Outer epidermis (Oep), inner epidermis (Iep), nucellar cuticle (Nct), nucellus (N), and endosperm (En) are enveloped by a tectum ("Tc"), excepting the fibrous structure (Fig. 9B). It follows that the preserved structural model of the coalified *T. grandis* ovule is organized as follows:

palisade—Oep—Iep—NCt—N—En—N—NCt—Iep—Oep—palisade.

We reinterpret Fig. 8A–C of Zodrow et al. (2013a) as a vascular bundle (see Taylor, 1965). The sequence tectum-nucellar cuticle-nucellus is demonstrated in a contiguous sample (Fig. 13).

4.3. Chemometrics

The 3D plot (Fig. 10) identifies changes in aromaticity, carbonyl (C═O) content related to cross-linking degree of macromolecular structures, and length and branching degree of aliphatic hydrocarbon-side chains, respectively. The implication is that changes in organic moieties of the structural components of the ovules are transitional, rather than sharply delineated. Noting exceptions, the epidermal samples (upper part of the plot) are characterized by high CH_2/CH_3 ratios (high aliphatic character), and oxygen-containing compounds. This implies longer and mainly linear (less branched) polymethylenic side chains, very low aromaticity, and the highest contents of oxygen-containing compounds. The latter includes C═O groups which are related to the formation of ester linkage, and consequently to an increased intermolecular cross-linking (i.e., more ester bonds implies higher cross-linking degree). Moreover, the nucellus occupies an intermediate composition between the epidermis/cutin and the vitrain, and the tectum and the fibers a somewhat in between composition with vitrain-like samples. The position of the tectum is uncertain because of possible error, as noted.

PCA scores (Fig. 11) clearly demonstrate chemical groupings of (a) nucellii, (b) epidermises, and (c) vitrain be it from the ovules or the Lloyd Cove Seam itself, whereas groupings for endospermous vis-à-vis integumentary epidermises are ambiguous. Exceptional scores are noted for (a) nucellus "Nuc3", (b) epidermal "Top", "261HF", "2614 h" "Carb", "Top12", and for "Tc" and "Fib", where "Nuc3" and "Top12" are likely random chemical variation as a function of sampling

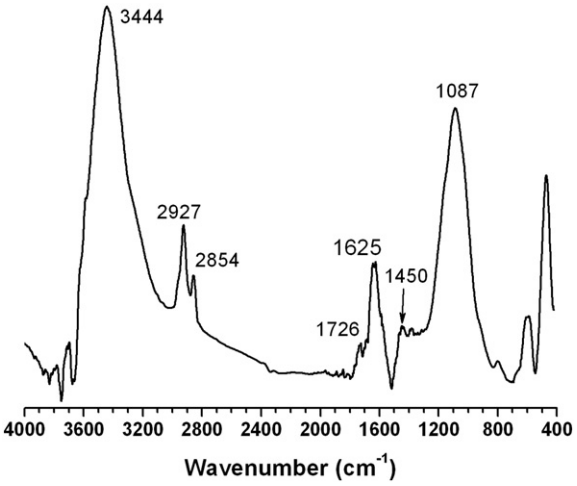

Fig. 14. *Trigonocarpus grandis* 3–309 ovule. IR spectrum of a tectum.

Table 6
IR characteristics of fibers and tectum, particularly in reference to polysaccharides.

Peak (cm^{-1})	Remarks	Peak (cm^{-1})	Remarks
Fibers: Fig. 9B1		Tectum: Fig. 14	
1717	C–O stretch, aliphatic ester	1726	C–O stretch, aliphatic ester
1634	C–O ketonic stretch, and likely Phenolic O═H stretch. C–O stretch Due to carboxylic acid and aldehyde	1625	C═O, H–O stretches of C═O in highly Conjugated ketonic structures, and H–O In phenolic compounds, respectively
1385	Doubtful organic, likely crystalline	1450	Antisymmetric deformation of CH_3 and CH_2 in aliphatic compounds
3465, 1093, 1022	Likely C–O stretches indicative of sugars	1087	Overlapping bands from 1294–833 cm^{-1}
		1094	C–O–H bending deformations in Amylose, amylopectin and starch.

position of the nucellus/epidermis (Fig. 3A). Such variation has also been observed in the nucellus of *Cycas rumphii* (Zodrow et al., 2013b).

Analogous to fossilized-cuticles (Zodrow and Mastalerz, 2009), macerating epidermal tissue is expected to increase the CH_2/CH_3 ratio (D'Angelo, 2006). This is not the case for the "fossilized-epidermis" from the 4-261ovule, where the CH_2/CH_3 ratio decreased from 7.9 in "261HF" (HF treated only) to 0.6 in "2614 h" that was macerated for 4 h. A likely explanation involves an unknown fossilization aspect that caused a low cross linking of polymeric structures (cf. CH_{al}/C═O; Zodrow et al., 2013a), resulting into a low CH_2/CH_3 ratio for "2614 h" which is chemically equivalent to vitrain ("V").

"Carb" (carbonate-like epidermis: Fig. 9E) disintegrated slowly during 4 h of maceration which is consistent with a sideritic composition. This is a potential expression for siderite coal-ball formation that is well-documented for Bolsovian strata (ex Westphalian C) of Nova Scotia and New Brunswick, Canada (Lyons et al., 1997). Coal balls have never been reported from the Sydney Coalfield, though siderite ("ironstone") is precipitated in coal seams, most abundantly as nodules or lenses in roof rocks (Zodrow, 1983). The nodules occasionally preserved plant remains similar to the Mazon Creek Flora of Illinois, USA (Darrah, 1969).

Vitrain, see (c) above, regardless whether from the Lloyd Cove Seam itself or from the 5-Lst#9 ovule, forms a vitrain grouping that probably reflects a common genetic history in the stratal sequence roof-rock–coal seam–seat rock (Zodrow et al., 2009, p.71). Common plant-source material is probably a contributing factor, considering the medullosalean forestation of the Lloyd Cove mire ca. 300 Ma ago.

Ostensibly, the scores of "Fib" (fibers: IR spectrum Fig. 9B1) and "Tc" (tectum: IR spectrum Fig. 14) pose difficulties for grouping because of the nature of their moietal contents (Table 6). Added is that the CH_2/CH_3 ratio for "Tc" is likely higher than the calculated value of 1.8 due to analytical error. But the two spectra show evidence for sugars (polysaccharides): "Fib" by the prominent absorption at 3465 cm^{-1} (O–H stretch) along with 1093 cm^{-1} and 1022 cm^{-1} (C–O stretches), and "Tc" by the absorption at 1087 cm^{-1} that is usually assigned to the C–O–H bending deformations in polysaccharide compounds, namely amylose, amylopectin, cellulose and starch. Polysaccharides are labile, relatively unstable molecules, and preservation of them in the fossil ovules is significant for chemotaxonomy (see Lyons et al., 1995; Zodrow et al., 2013a). An unrecognized fossilization process was probably involved in the preservation.

4.4. Mass- to-charge ratios

The difficulty in dealing with electrospray ionization in the ASAP probe is twofold. One is the lack of a comprehensive library to help identifying compounds, and the other is that nucellar and epidermal samples of 3–309 ovule represent mixtures. We assume that the mixtures comprise waxes and non-structure matrix analogous with the extant foliar cuticle well-described in the literature (e.g., Koch and Ensikat, 2008). Our initial model for m/z interpretation is the structure of the cutin-building block (Van Bergen et al., 2004, Fig. 8.6), with an approximate empirical formula of $C_{17}H_{29}O_5$ R_2, or 313 + R_2 atomic mass units (amu). The polymeric structure is formed by a chain-like repetition of this block, which in the case of the nucellar m/z spectrum, assumes an empirical formula approximated by 353 amu. Evidence for a hydrocarbon-chain structure is known from powder X-ray diffraction of the nucellus of the Ovxx2 ovule (Lin et al., 2013). The crucial assumption for the m/z's 113, 120, and 125 of the nucellus is that they represent ionic fragments of the cutin-building block, or ionic molecule. The epidermal spectrum (170–209 amu) highlights the interpretive challenge, but brings to the fore that the data have a structure testable by factor-analytic methods (Zodrow, 1991). PCA scores, which separate the epidermis from the nucellus (Fig. 11), seem to signal as much.

A lignin formula $C_9H_{10}O_2$ is hypothesized for the vitrain from the Lloyd Cove Seam and the 3–309 ovule (pers. comm. July, 2013, Dr. M. Mastalerz). The virtual identity of m/z ratios confirms the genetic relationship between coal-seam and coalified- ovule vitrain as hypothesized by Lyons et al. (1995), based on ^{13}C NMR analysis. However, we mention that our m/z interpretations are necessarily preliminary to be up-dated in a future publication in which we present results from isotopically modeling the cutin-building block, based on more data D'Angelo and Zodrow (2013).

4.5. Aliphatics and preservation

With certain exceptions, namely "V" vitrain and macerated "2614 h", all other structural variables show relatively high CH_2/CH_3 values. In the 2–336 IR data, the nucellar and epidermal average ratios (aliphatic content) are identical. But the Py-GC/MS analyses of the three nucellii show the clearest evidence yet for lipid residue, which bears resemblance to the epicuticular waxes of extant cuticles (summary: Koch and Ensikat, 2008). Complementing the nucellar results is the epidermal analysis of 8-ovule of *T. grandis* from the Lloyd Cove Seam which shows a normal *n*-alkene/*n*-alkane series (Zodrow et al., 2013a, Fig. 10A). These two structures have similar profiles, although the column and final temperatures used for the present nucellar analyses do not show the higher carbon numbers as are shown for 8-ovule. Specifically, both the previously published epidermal and the present nucellar analyses have (a) only C_4 to C_{10} in common, (b) but the same ene/ane profiles for C_{15} up. The only difference is for C_{11}–C_{14}, and in the epidermis of 8-ovule where an ene/ane pairing exists, whereas in the nucellii there are C_{11} ane, C_{12} ane C_{13} ene, and C_{14} ane. The ratio alkene/alkane for the present nucellii is 0.73, whereas that for the epidermis is approximately 3 ~ 1. ^{13}C NMR data, without being able to quantify it, confirm unequivocally aliphatic-carbon dominance for the Ovxx2 nucellus (═Ov19d, Table 3) (Lin et al., 2013).

We have demonstrated the aliphatic nature for the structure/tissue components, excepting nucellar cuticles which, however, we assume aliphatic as well. The inference is that aliphatics (lipids as lipoidic waxes) are factors to the extent that structure/tissue preservation depends on them, but not entirely. The influence of lithology was recognized by Darrah (1969, p. 67) who suggested a "… relationship between environment of sedimentation and preservation of plant

debris." This, in terms of facies changes, is reflected in the organic-matter transformation of the seed to the 3D [type(ii)] ovule, which still shows aspects of coalification, but acellular preservation.

4.6. Advancing medullosalean systematics

According to Nip et al. (1989), Villena et al. (2000) and others, extant plant cuticles in their structural make-up also contain polysaccharides. Thus, the analytical signature of fossil cutin does not reside in the methylene/methyl ratio alone, but also in "sugar fingerprints". To this we add the data from powder X-ray diffraction analysis of the Ovxx2 nucellus (= Ov19d, Table 3) that compares (Lin et al., 2013) with cutin (waxes) as reported by Stoyko et al. (2013, and references there in). Thus, we assume the existence of a cutin structure, although with possible differences between the epidermis and the nucellus, i.e., as different mixtures. Another important experimental development to consider is Koch and Ensikat's (2008) demonstration of lipid chemistry (waxes) and species dependency in extant cuticles, which we assume is applicable to fossil ovules as well. The process for nucellar cutin adds weeks for obtaining result, but it has the advantage that the prolonged maceration oxidized "…all available chemical species and the final products are presumably determined by the original structure of the plant." (Zodrow et al., 2013a). This is a crucial preliminary development for advancing the stalled systematics of Carboniferous medullosalean ovules.

5. Concluding remarks

Demonstrated is that coalified medullosalean *T. grandis* ovules are an invaluable information source, complementing coal-ball petrification. Type(i) coalification particularly signifies optimal preservation conditions for the structure/tissue components, considering the aliphatic (lipid) nature of the original Carboniferous seeds. This does not imply that aliphatic chemistry guarantees preservation because the natural threshold at which this happens remains unknown, the chemistry is probably structure-dependent, and sedimentary environments may interfere with organic-matter transformation to type(i) coalified ovule. Nevertheless, species-dependent nucellar-cutin is hypothesized for advancing chemotaxonomy/systematics of medullosalean ovules. The elevation of the coalified *T. grandis* ovule to a general model depends on confirmative results from the larger coalified species in other Carboniferous coalfields. A future paper will deal with questions of the monophylogeny and evolution of Cycadophytes. Particularly considering the latter, the seed of *Cycas rumphii* is first-time compared with *T. grandis* via morphology, structure, and histochemistry combined.

Presently, we are experimenting how most efficiently to assess prolonged nucellar maceration products for concentrating cutin by methods of FTIR, Py-GC/MS, powder X-ray diffraction analysis, and mass spectrometry. Moreover, statistical aspects of the presented PCA analysis are more fully analyzed in a future paper in which a structure for the data is hypothesized.

Acknowledgments

Microscopes for Nomarski phase-contrast study, and the infrared spectrometer were made available to ELZ by M. Katherine Jones (Biology Department) and D. Keefe (Molecular Spectroscopy Research Laboratory, Department of Chemistry), respectively; moreover, J. MacInnis produced the m/z data and together with A. Britten (Department of Chemistry) suggested interpretation; all of Cape Breton University; A. Mar, R.E. Wasylishen, and co-workers provided the X-ray and ^{13}C NMR data (Chemistry Department, University of Alberta); M. Mastalerz (Indiana Geological Survey, Indiana University) analyzed the tectum sample, measured vitrinite reflectance, donated samples of the Indiana paper coal, and helped with the interpretation of m/z data; M. R. Gibling (Department of Earth Sciences, Dalhousie University) contributed thin-section analysis (Harbour Seam); D. Stevenson (New York Botanical Garden) donated *Cycas rumphii* seeds; and W. DiMichele (Smithsonian Institution, Washington, D.C.) made valuable suggestions concerning the physiological function of tectum. Presentation and technical contents were thoughtfully improved by the two anonymous journal reviewers. We are much obliged and most grateful to our colleagues for their time and efforts dedicated in supporting the MS.

Appendix A. Supplementary data

Supplementary data to this article can be found online at http://dx.doi.org/10.1016/j.coal.2013.12.008.

References

Almendros, G., Zancada, M.C., González-Vila, F.J., Lesiak, M.A., Alvarez-Ramis, C., 2005. Molecular features of fossil organic matter in remains of the Lower Cretaceous fern *Weichselia reticulata* from Przenosza basement (Poland). Org. Geochem. 36, 1108–1115.
Arnold, C.A., 1948. Some cutinized seed membranes from the coal-bearing rocks of Michigan. Bull. Torrey Bot. Club 75, 131–146.
Bell, W.A., 1938. Fossil flora of Sydney Coalfield, Nova Scotia. Geol. Surv. Mem. 215, 334.
Bell, W.A., 1962. Catalogue of types and figured specimens of fossil plants in the Geological Survey of Canada. Geological Survey of Canada, Ottawa 154.
Benítez, J.J., Matas, A.J., Heredia, A., 2004. Molecular charaterization of the plant biopolyester cutin by AFM and spectroscopic techniques. J. Struct. Biol. 147, 179184.
Cheng, Y., Mastalerz, M., Schimmelmann, A., 2012. Characterization of chemical functional groups in macerals across different coal ranks via micro-FTIR spectroscopy. Int. J. Coal Geol. 104, 22–33.
Cleal, C.J., Shute, C.H., 2012. The systematic and palaeoecological value of foliage anatomy in Late Palaezoic medullosalean seed-plants. J. Syst. Palaeontol. 10, 765–1800.
Cleal, C.J., Zodrow, E.L., Mastalerz, M., 2010. An association of *Alethopteris* foliage, *Trigonocarpus* ovules and *Bernaultia*-like pollen organs from the Middle Pennsylvanian of Nova Scotia, Canada. Palaeontogr. B 283, 73–97.
D'Angelo, J.A., 2006. Analysis by Fourier transform infrared spectroscopy of *Johnstonia* (Corystospermales, Corystospermaceae) cuticles and compressions from the Triassic of Cacheuta, Mendoza, Argentina. Ameghiniana 43, 669–685.
D'Angelo, J.A., Zodrow, E.L., 2011. Chemometric study of functional groups in different layers of *Trigonocarpus grandis* ovules (Pennsylvanian seed fern, Canada). Org. Geochem. 42, 1039–1054.
D'Angelo, J.A., Zodrow, E.L., 2013. Cutin in the Carboniferous fossil record: what new evidence is there? MS.
D'Angelo, J.A., Lyons, P.C., Mastalerz, M., Zodrow, E.L., 2013. Fossil cutin of *Macroneuropteris scheuchzeri* (Late Pennsylvanian seed fern, Canada). Int. J. Coal Geol. 105, 137–140.
Darrah, E.L., 1968. The microstructure of some Pennsylvanian seeds and megaspores studied by maceration. Micropaleontology 14, 87–104.
Darrah, W.C., 1969. A critical review of the Upper Pennsylvanian floras of Eastern United States with notes on the Mazon Creek flora of Illinois (Self published, pp. 220, plus 1–80 plates).
Dawson, J.W., 1868. Acadian geology, 2nd revised ed. MacMillan and Co., London 694 (enlarged).
De Sloover, J.-L., 1964. Etudes sur les Cycadales – III Nucelle, Gamétophyte Femelle et Embryon (*Encephalartos poggei* Asch. Cellule 64, 149–200.
Deevers, Ch., 1937. Structure of Paleozoic seeds of the Trigonocarpales. Bot. Gaz. 98, 572–585.
Doubinger, J., Vetter, P., Langioux, J., Galtier, J., Broutin, J., 1995. La flore fossile du basin houiller de Saint-Étienne. Mémoirs du Muséum National D'Histoire Naturelle 164, Paris. 355.
Edwards, D., Ewbank, G., Abbott, G.D., 1997. Flash pyrolysis of the outer cortical tissue in Lower Devonian Psilophyton dawsonii. Bot. J. Linn. Soc. Lond. 124, 345–360.
Ganz, H., Kalkreuth, W., 1987. Application of infrared spectroscopy to the classification of kerogen-types and the evolution of source rock and oil–shale potentials. Fuel 66, 708–711.
Gastaldo, R.A., Matten, L.C., 1978. Trigonocarpus leeanus. A new species from the Middle Pennsylvanian of Southern Illinois. Am. J. Bot. 65, 882–890.
Hacquebard, P.A., 1993. The Sydney coalfield of Nova Scotia, Canada. Int. J. Coal Geol. 23, 29–42.
Herr Jr., J.M., 1995. The origin of the ovule. Am. J. Bot. 82, 547–564.
Hooker, J.D., Binney, E.W., 1855. On the structure of certain limestone nodules enclosed in seams of bituminous coal, with a descriptions of some trigonocarpons contained in them. Philos. Trans. R. Soc. Lond. 145 (1), 149–156.
Hoskins, J.H., Cross, A.T., 1946a. Studies in the Trigonocarpales. Pt. II. Taxonomic problems and a revision of the genus *Pachytesta*. Am. Midl. Nat. 36, 331–361.
Hoskins, J.H., Cross, A.T., 1946b. Studies in the Trigonocarpales. Pt I. *Pachytesta vera*, a new species from the Des Moines Series of Iowa. Am. Midl. Nat. 36, 207–250.
Kerp, H., 1990. The study of fossil gymnosperms by means of cuticular analysis. Palaios 5, 548–569.
Koch, K., Ensikat, H.-J., 2008. The hydrophobic coatings of plant surfaces: Epicuticular wax crystals and their morphologies, crystallinity and molecular self-assembly. Micron 39, 759–772.
Koch, K., Bhushan, B., Barthlott, W., 2009. Multifunctional surface structures of plants: an aspiration for biomimetics. Prog. Mater. Sci. 54, 137–178.
Kolattukudy, P.E., 2002. Cutin from plants. In: Biopolymers, Volume 13a, Polyesters 1: Biological Systems and Biotechnological Production. Volume editors: Y. Doi and A. Steinbuchel; Wiley-VCH, p. 472.

Lin, R., Ritz, G.P., 1993a. Reflectance FT-IR microspectroscopy of fossil algae contained in organic-rich shale. Appl. Spectrosc. 47, 265–271.
Lin, R., Ritz, G.P., 1993b. Studying individual macerals using i.r. microspectroscopy, and implications on oil versus gas/condensate proneness and "low-rank" generation. Org. Geochem. 20, 695–706.
Lin, X., Mar, A., Bernard, G.M., Wasylishen, R.E., 2013. Powder X-ray diffraction and solid-state ^{13}C NMR spectroscopy of a megaspore membrane of *Trigonocarpus grandis* (coalified tree-fern ovule, Sydney, Coalfield, Canada). MS.
Lyons, P.C., Orem, W.H., Mastalerz, M., Zodrow, E.L., Vieth-Redemann, A., Bustin, R.M., 1995. ^{13}C NMR, micro-FTIR and fluorescence spectra, and pyrolysis-gas chromatograms of coalified foliage of late Carboniferous medullosan seed ferns, Nova Scotia, Canada: implications for coalification and chemotaxonomy. Int. J. Coal Geol. 27, 227–248.
Lyons, P.C., Zodrow, E.L., Millay, M.A., Dolby, G., Gillis, K.S., Cross, A.T., 1997. Coal-ball floras of Maritime Canada and palynology of the Foord Seam: geologic, palaeobotanical, and palaeoecological implications. Rev. Palaeobot. Palynol. 95, 31–50.
Mastalerz, M., Bustin, R.M., 1997. Variation in chemistry of macerals in coals of the Mist Mountain Formation, Elk Valley coalfield, British Columbia, Canada. Int. J. Coal Geol. 33, 43–59.
Merk, S., Blume, E., Riederer, M., 1998. Phase behavior and crystallinity of plant cuticular waxes studied by Fourier transform infrared spectroscopy. Planta 204, 44–53.
Mosbrugger, V., 1989. Gibt es sprunghafte Evolution? Biol. unserer Zeit 19, 1–8.
Neavel, R.C., Miller, L.V., 1960. Properties of cutinite. Fuel 39, 217–222.
Nip, M., De Leeuw, J.W., Schenk, P.A., Windig, W., Meuzelaar, H.L.C., Crelling, J.J., 1989. A flash pyrolysis and petrographic study of cutinite from the Indiana paper coal. Geochim. Cosmochim. Acta 53, 671–683.
Norstog, K.J., Nicholls, T.J., 1997. The biology of the cycads. Comstock Publishing Associates, Ithaca, N.Y. 363.
Novoselov, N.P., Sashina, E.S., Kuz'mina, O.G., Troshenkova, S.V., 2007. Ionic liquids and their use for the dissolution of natural polymers. Russ. J. Gen. Chem. 77, 1395–1405.
Oliver, F.W., Scott, D.H., 1904. On the structure of the Palaeozoic seed *Lagenostoma lomaxi*, with a Statement Of Evidence upon which it is referred to *Lyginodendron*. R. Soc. Philos. Trans. B 197, 193–247 (plus pls. 4–10).
Pavia, D.L., Lampman, G.M., Kriz, G.S., Vyvyan, J.R., 2009. Introduction to spectroscopy, 4th ed. Brooks/Cole, USA 656 (plus Appendices).
Petersen, H.I., Nytoft, H.P., 2006. Oil generation capacity of coals as a function of coal age and aliphatic structure. Org. Geochem. 37, 558–583.
Reed, F.D., 1939. Structure of some Carboniferous seeds from American coal fields. Bot. Gaz. 100, 769–787.
Stopes, M.C., 1905. On the double nature of the cycadean integument. Ann. Bot. 19, 561–566.
Stopes, M.C., 1919. On the four visible ingredients in banded bituminous coal: studies in the composition of coal, No. 1. Proc. R. Soc. B 90, 470–487.
Stoyko, S., Rudyk, B.W., Mar, A., Zodrow, E.L., D'Angelo, J.A., 2013. Powder X-ray diffraction and X-ray photoelectron spectroscopy of cutin from a 300 Ma tree fern (*Alethopteris pseudograndinioides*, Canada). Int. J. Coal Geol. 106, 35–38.
Taylor, T.N., 1965. Paleozoic seed studies: a monograph of the American species of *Pachytesta*. Palaeontogr. B 117, 1–46.
Teacă, C., Bodîrlău, R., Spiridon, I., 2011. Dissolution of natural polymers in ionic liquid. Rev. Roum. Chim. 56, 33–38.
Thomas, B.A., Spicer, R.A., 1987. The evolution and palaeobiology of land plants. Croom Helm, London 309.
Truernit, E., Haseloff, J., 2008. *Arabidopsis thaliana* outer ovule integument. morphogenesis: Ectopic expression of KNAT1 reveals a compensation mechanism. BMC Plant Biol. 8:35. http://dx.doi.org/10.1186/1471-2229-8-35.
Van Bergen, P.F., Collinson, M.E., Sinninghe Damsté, J.S., de Leeuw, J.W., 1994. Chemical and macroscopical characterization of inner seed coats of fossil water plants. Geochim. Cosmochim. Acta 58, 231–239.
Van Bergen, P.F., Blokker, P., Collinson, M.E., Sinninghe Damsté, J.S., de Leeuw, J.W., 2004. Structural biomocromolecules in plants: what can be learnt from the fossil record? In: Hemsley, A.R., Poole, I. (Eds.), The Evolution of Plant Physiology. Elsevier Academic Press, Oxford, pp. 133–154.
Villena, J.F., Domínguez, E., Heredia, A., 2000. Monitoring biopolymers present in plant cuticles by FI-IR. J. Plant Physiol. 156, 419–422.
White, D., 1899. Fossil flora of the Lower Coal Measures of Missouri. Monogr. U.S. Geol. Surv. 37, 467.
Zimmerman, R.P., Taylor, T.N., 1970. The ultrastructure of Paleozoic megaspore membranes. Pollen Spores 12, 451–468.
Zodrow, E.L., 1983. Some geochemical aspects of sedimentary rocks in proximity of coals, Sydney Coalfield (Upper Carboniferous), Cape Breton Island, Nova Scotia, Canada. Int. J. Coal Geol. 2, 299–320.
Zodrow, E.L., 1991. A coal–sulfur model for Sydney Coalfield (Upper Carboniferous), Nova Scotia, Canada. Atl. Geol. 27, 127–142.
Zodrow, E.L., 2002. The "medullosalean forest" at the Lloyd Cove Seam (Pennsylvanian, Sydney Coalfield, Nova Scotia). Atl. Geol. 38, 177–195.
Zodrow, E.L., 2004. Note on different kinds of attachments in trigonocarpalean (Medullosales) ovules from the Pennsylvanian Sydney Coalfield, Canada. Atl. Geol. 40, 197–206.
Zodrow, E.L., 2007. Reconstructed tree fern *Alethopteris zeilleri* (Carboniferous, Medullosales). Int. J. Coal Geol. 69, 68–89.
Zodrow, E.L., D'Angelo, J.A., 2013. Digital compression maps: an improved method for studying Carboniferous foliage. Atl. Geol. 49, 126–130.
Zodrow, E.L., Mastalerz, M., 2001. Chemotaxonomy for naturally macerated tree-fern cuticles (Medullosales and Marattiales), Carboniferous Sydney and Mabou Sub-Basins, Nova Scotia, Canada. Int. J. Coal Geol. 47, 255–275.
Zodrow, E.L., Mastalerz, M., 2009. A proposed origin for fossilized Pennsylvanian plant cuticles by pyrite oxidation (Sydney Coalfield, Nova Scotia, Canada). Bull. Geosci. 84, 227–240.
Zodrow, E.L., D'Angelo, J.A., Mastalerz, M., Keefe, D., 2009. Compression-cuticle relationship of seed ferns: Insights from liquid–solid FTIR (Late Palaeozoic–Early Mesozoic, Canada–Spain–Argentina). Int. J. Coal Geol. 79, 61–73.
Zodrow, E.L., D'Angelo, J.A., Helleur, R., Simůnek, Z., 2012. Functional groups and common pyrolysates products of *Odontopteris cantabrica* (index fossil for the Cantabrian Substage, Carboniferous). Int. J. Coal Geol. 100, 40–50.
Zodrow, E.L., Helleur, R., Werner-Zwanziger, U., Chen, B., D'Angelo, J.A., 2013a. Spectrochemical study of coalified *Trigonocarpus grandis* (Pennsylvanian tree-fern ovule, Canada): Implications for fossil–organ linkage. Int. J. Coal Geol. 109–110, 24–35.
Zodrow, E.L., D'Angelo, J.A., Al-Shra'ah, A., 2013b. The seed of *Cycas rumphii* as a model for the larger Carboniferous medullosalean ovules. Implication for cycadean evolution. MS in progress.